Force-velocity relationship in cycling revisited: benefit of two-dimensional pedal forces analysis

Sylvain Dorel, Antoine Couturier, Jean-René Lacour, Henry Vandewalle, Christophe Hautier, François Hug

Force-velocity relationship in cycling revisited: benefit of two-dimensional pedal forces analysis

Sylvain Dorel [1], Antoine Couturier [1], Jean-René Lacour [2], Henry Vandewalle [3], Christophe Hautier [2], and François Hug [1,4]

[1] Laboratory of Biomechanics and Physiology, Research Department, National Institute for Sports and Physical Education (INSEP), Paris, FRANCE;
[2]INRETS, University Claude Bernard Lyon 1, Oullins, FRANCE;
[3] Department of Functional Explorations and Sports Medicine, AP-HP Avicenne Hospital, Bobigny, FRANCE;
[4]Laboratory Motricité, Interactions, Performance, University of Nantes, Nantes, FRANCE

Address for correspondence: Sylvain Dorel, Ph.D., Research Department, Laboratory of Biomechanics and Physiology (LBP-SPE), National Institute for Sports and Physical Education (INSEP), 11 Avenue du Tremblay, 75012, Paris, France; E-mail: sylvain.dorel@hotmail.fr; sylvain.dorel@ univ-nantes.fr.

Article publié dans *: Medicine & science in sports & exercise, 2010, vol.42, n°6, pp. 1174-1183 (DOI : 10.1249/MSS.0b013e3181c91f35)*

ABSTRACT

Purpose: Maximal cycling exercise has been widely used to describe the power-velocity characteristics of lower-limb extensor muscles. This study investigated the contribution of each functional sector (i.e., extension, flexion, and transitions sectors) on the total force produced over a complete pedaling cycle. We also examined the ratio of effective force to the total pedal force, termed index of mechanical effectiveness (IE), in explaining differences in power between subjects.

Methods: Two-dimensional pedal forces and crank angles were measured during a cycling force-velocity test performed by 14 active men. Mean values of forces, power output, and IE over four functional angular sectors were assessed: top = 330°-30°, downstroke = 30°-150°, bottom = 150°-210°, and upstroke = 210°-330°.

Results: Linear and quadratic force-velocity and power-velocity relationships were obtained for downstroke and upstroke. Maximal power output *($P_{max,,}$)* generated over these two sectors represented, respectively, 73.6% ± 2.6% and 10.3% ± 1.8% of P_{max} assessed over the entire cycle. In the whole group, P_{max} over the complete cycle was significantly related to P_{max} during the downstroke and upstroke. IE significantly decreased with pedaling rate, especially in bottom and upstroke. There were significant relationships between power output and IE for top and upstroke when the pedaling rate was below or around the optimal value and in all the sectors at very high cadences.

Conclusions: Although data from force-velocity test primarily characterize the muscular function involved in the downstroke phase, they also reflect the flexor muscles' ability to actively pull on the pedal during the upstroke. IE influences the power output in the upstroke phase and near the top dead center, and IE accounts for differences in power between subjects at high pedaling rates.

Key Words: maximal power output, index of effectiveness, cycling biomechanics, muscular function, sprint cycling

All-out exercise on cycle ergometer has been widely used over the last three decades to evaluate muscle power characteristics (1,8,15,21,32,35). Linear and polynomial relationships can be obtained, respectively, between the force (effective component on the pedal or torque at the crank axis) and the pedaling rate and between the power output and the pedaling rate. These relationships permit the assessment of useful parameters, including (i) maximal pedaling rate at the zero force axis (f_0), (ii) maximal force at a zero pedaling rate *(F_{eff0}),* (iii) maximum value of power output *(P_{max}),* and (iv) optimal pedaling rate (f_{opt}) corresponding to the value at which P_{max} is reached. Some of these parameters have been directly linked to performance. For example, short sprint running (initial running speed between 5 and 10 m or 60-m time performance) has been reported to be positively correlated with P_{max} normalized to body mass (3,22). In addition, vertical jumping has been related to P_{max} (35) and f_{opt} (14). More recently, Dorel et al. (8) established that both P_m normalized to the frontal area and f_{opt} were significant predictors of the 200-m sprint cycling performance in world clans cyclists. These findings support the hypothesis that P_{max} could accourt for the leg muscle function, especially the knee extensors. Driss et al. (9) reported strong relationships between F_{eff0} and P_{max} obtained during a cycling task and strength indices measured during the knee extension (i.e., the rate of isometric force development and the peak knee extension torques at high velocities). The link between the optimal pedaling rate (or the maximal theoretical pedaling rate) and the fiber-type composition of knee extensors has been assumed by several authors (8,32,35) and was demonstrated for the *vastus lateralis* muscle by Hautier et al. (14). On the basis of these findings, maximal cycling is considered by the scientific community as a useful testing procedure to evaluate the human dynamic muscle function.

From a biomechanical point of view, pedaling is a multijoint cyclic movement of the lower extremity that requires specific coordination of the lower-limb muscles (16). This coordination strategy results in the effective force profile along a complete crank cycle that is relatively stereotypical during a submaximal exercise. A large positive contribution to total force production during the downstroke phase and a slight negative contribution in the upstroke phase are commonly observed (7,12,31). However, an increase in power output decreases the peak negative force and negative impulse measured during the upstroke phase (27,31). An increase in intensity to the maximal aerobic power leads to an increasing contribution from all the flexor muscles involved in the pull-up action during the second part of the cycle (from 180° to 360°) (11,23). As recently described by Martin and Brown (19), an even more pronounced contribution of the upstroke phase appears during a maximal isokinetic cycling. To the best of our knowledge, no previous study using a conventional cycle ergometer has focused on the force produced in the different parts of the pedaling cycle and its relationship to pedaling rate during an all-out cycling exercise, such as the force-velocity test.

Pedaling techniques can be characterized by the ability to efficiently orient the total force on the pedal. The index of mechanical effectiveness (IE) was defined as the ratio of the effective force to the total force exerted at the shoe-pedal interface during a complete cycle (18,29). As far as we know, there is no information in the literature on the index of mechanical effectiveness during this type of explosive cycling exercise. A few studies (4,5) have investigated the torque profile at very high pedaling rates without exploring mechanical effectiveness. During submaximal exercise, IE has been reported to increase significantly with workload because of its increase during the upstroke phase (6,26,27,36). For a given submaximal power, an increase in pedaling rate is known to reduce the effective force produced in the upstroke phase and in the mechanical effectiveness (25,31). Although these studies are restricted to submaximal exercise, these findings suggest that this index may be useful when interpreting (i) the force and power changes associated with the increase in pedaling rate during the force-velocity test and (ii) the differences in maximal power capacity among subjects.

The present study examines whether further information about two-dimensional biomechanics of pedaling could provide some new insight on muscle force and power characteristics measured by the cycling force-velocity test. Although this test is classically used to assess the muscle function of the knee extensors, the actual participation of these muscle groups compared with the others has not been fully evaluated. It is also not known what effect pedaling technique has on biomechanical and force transmission parameters.

Therefore, the purpose of this study was to investigate the contribution of each functional phase of the crank cycle and the influence of the pedaling technique on power output produced during a maximal cycling sprint. We hypothesized that cycling force-velocity characteristics reflect not only the muscle function of the extensors acting during the downstroke but also the muscle's ability to pull up the pedal during the upstroke and to orientate efficiently the total force on the pedal.

MATERIALS AND METHODS

Subjects. Fourteen healthy active male subjects volunteered to take part in this study (mean ± SD: age = 29.2 ± 5.5 yr; stature = 1.77 ± 7.1 m; body mass = 69.7 ± 7.6 kg; body mass index = 22.1 ± 1.4 kg•m^{-2}). They were engaged in leisure sport activity (three in team sport, two in triathlon, two in athletics, three in cycling, three in multiactivity, and one in climbing). All subjects were instructed to refrain from intense physical activities during the 2 d before testing. The study was conducted in accordance with the Declaration of Helsinki and approved by the ethics committee of Saint-Germain-en-Laye (France; acceptance No. 06016). An informed consent was obtained from all participants before inclusion.

Exercise protocol. Subjects exercised on an electronically braked cycle ergometer (Excalibur Sport; Lode®, Groningen, The Netherlands). Vertical and horizontal positions of the saddle, handlebar height, and stem length were set to match the most comfortable and usual position of the participants (i.e., "racing" or "dropped" posture). A standard crank length of 170 mm (similar or close to the crank length used in the field) was chosen to provide classical test conditions. The session began with a 20-min warm-up consisting of 12 min of pedaling at a power output of 100-150 W followed by two brief sprints (3- to 5-s duration, separated by 4 min of recovery) against high and low resistance.

After this warm-up, the participants were asked to perform three maximal cycling sprints of 5-s duration, interspersed with 5-min rest periods. According to the torque—velocity protocol proposed by Arsac et al. (1) and Dorel et al. (8), each sprint was performed against a specific resistance applied to the flywheel in a randomized order. The corresponding resistive torques were 0, 0.5, and 1 N•m•kg^{-1} body mass and were chosen to allow subjects to attain a large range of pedaling rates among the three bouts. Before starting the zero load sprint, subjects pedaled until the flywheel turned at 80-90 rpm. The beginning of the sprint occurred alter 20 s of passive rest period, during which the flywheel kept turning at this velocity. This procedure reduced the acceleration phase and made it possible to briefly reach a high level of pedaling rate without fatigue. During the maximal effort, subjects were told to remain seated on the saddle and were vigorously encouraged to produce the highest acceleration possible.

Materials and data collection. The cycle ergometer was equipped with instrumented pedals specifically designed for measuring pedal loads (VélUS group; Department of Mechanical Engineering, Sherbrooke University, Canada) and previously described elsewhere (Fig. 1) (7,10,17). These instrumented pedals were used with the LOOK CX7 clipless platform (using LOOK Delta cleat) or the Shimano 600 toe-clip and strap platform (model PD-6400, Shimano Inc., Osaka, Japan). Briefly, the sagittal plane components of the total reaction force (F_{tot}) applied at the shoe-pedal interface were measured using a series of eight strain gauges located within each pedal. F_{tot} was calculated from the measured Cartesian components F_T and F_N, corresponding to the horizontal forward and vertical upward forces on the pedal, respectively. An optical encoder with a resolution of 0.4° mounted on the pedal measured pedal angle (13) with respect to the crank orientation. Zero adjustments for both components of force and pedal angle were done before each session. The crank angle (0) was calculated on the basis of transistor-transistor logic (TTL) pulses delivered each 2° by the cycle ergometer. Additional TTL pulses allowed the detection of the bottom dead center (BDC) of the left pedal (i.e., lowest position of the left pedal with crank arm angle 180°). All these data were digitized at a sampling rate of 1 kHz (USB data acquisition; ISAAC Instruments®, Québec, Canada) and stored on a computer.

Data processing. All mechanical data were analyzed with two custom-written scripts (MATLAB, MathWorks®, Natcik, MA; and Origin 8, OriginLab Corporation®, Northampton, MA). On the basis of the F_N and F_T components and pedal angle (β), the total resultant force (F_{tot}) was calculated by trigonometry and resolved into two components: one propulsive and applied perpendicularly to the crank arm (F_{eff}, effective force) and one nonpropulsive and applied along the crank ineffective force) (Fig. 1). All data were smoothed by a 10-Hz third-order Butterworth low-pass filter and resampled (one value per degree) to get representative mechanical profiles as a function of the crank angle for each pedal (Figs. 1 and 2).

The angular velocity of the crank and the linear velocity of the pedal were calculated by derivative of the crank angle. Effective force, pedaling rate, and power output (product of effective force by linear velocity of the pedal) were averaged over each complete cycle. The overall index of mechanical effectiveness on the complete crank cycle (IE) was determined as the ratio of the linear impulse of F_{eff} to the linear integral of F_{tot} (7,18,30). A typical example of the force profiles is depicted on Figure 2A (IE 75.2% for mean value of F_{eff} (702 N) and F_{tot} (934 N) at 80 rpm). After computation, the data for both pedals and the three resistances were compiled and used to draw up the force-velocity and power-velocity relationships for each subject, using a linear and a second-order polynomial regression, respectively (8,15,32). Both maximal pedaling rate (f_o, in revolutions per minute) and maximal effective force (F_{eff0}, in newtons) were obtained by extrapolation. They corresponded to the intercept of the force-velocity linear relationship with the velocity and force axes, respectively. Maximum power (P_{mo}) was identified as the apex of the power-velocity relationship, and optimal pedaling rate (f_{opt}) corresponded to the specific value at which P_{max} occurred.

Mean values of the mechanical variables (F_{eff}, F_{tot}, power output, and IE) corresponding to four functional angular sectors of the pedaling cycle were calculated (7,17): sector 1, 330°-30° (top); sector 2, 30°-150° (downstroke); sector 3, 150°-210° (bottom); and sector 4, 210°-330° (upstroke) (with 0° corresponding to the highest position of the pedal). From a functional standpoint, sectors 1 and 3 correspond to the sectors around the top and the bottom dead centers (TDC and BDC), respectively, and sectors 2 and 4 correspond to the main propulsive downstroke and upstroke phases, respectively (Fig. 1). The values of force and power output for the different sectors were weighted regarding the size of each one relative to the entire cycle for each pedal (i.e., 60/360 for top, 120/360 for downstroke, 60/360 for bottom, and 120/360 for upstroke). Finally, depending on the sector considered and when it was suitable (see Statistical analysis section), similar procedures for force-velocity and power-velocity relationship plotting and for f_o, F_{eff0}, and P_{max} calculations were done on each sector.

Statistical analysis. All analyses were performed with OriginPro8 software for Windows (Origin 8; OriginLab Corporation®). Data were first tested for normality using the Kolmogorov-Smirnov test, and results were thereafter expressed as mean ± SD. When they were suitable ($P < 0.05$), linear and quadratic regression models were used to fit (least chi-square method, using the Levenberg-Marquardt algorithm) the evolution of the different mechanical variables according to the pedaling rate. The choice of the polynomial order was done according to a comparison algorithm of fit models (OriginPro8 software) and according to a significant increase of R^2 (Student's t-test). Pearson product-moment correlation coefficients were calculated to determine whether, on the whole sample ($N = 14$), relationships between mechanical variables obtained on the complete cycle and on each sector were significant and to test the influence of the index of mechanical effectiveness on the power output produced in all the sectors. Significant relationships between variables were examined with a level of significance set at $P < 0.05$.

RESULTS

Force, power output, and index of mechanical effectiveness: influence of pedaling rate. A typical recording of the effective and total forces exerted on one pedal during the complete cycle at three pedaling rates (i.e., low = 80 rpm, medium = 117 rpm, i.e., f_{opt}, and high = 170 rpm) is depicted in Figure 2. The linear effective forcepedaling rate relationships (mean R^2 = 0.983 ± 0.011) and quadratic power output-pedaling rate relationships (mean R^2 = 0.948 ± 0.042) on the complete cycle for the whole group are illustrated by Figure 3. Mean values of maximal and optimal cycling rates (f_o and f_{opt}), maximal effective force (F_{eff0}), and maximal power output (P_{max}) were 236 ± 11 rpm, 117 ± 5 rpm, 1063 ± 99 N, and 1132 ± 97 W,

respectively. Values of force (total and effective), pedaling rate, and power output averaged on the complete cycle and on the different sectors were normalized relative to the mean maximal values on the complete cycle (i.e., F_{eff0}), f_0, and P_{max}). In the whole group, the evolutions of F_{tot} and IE as a function of the pedaling rate on the complete cycle were best described by quadratic models (Fig. 3). The relationships between the mechanical parameters and the pedaling rate for each functional sector (described by linear or quadratic model, see Materials and methods section) are depicted in Figure 4. The mean values of the individual coefficients of determination (mean R^2) are specified for each of them in Figure 4. Effective force-velocity and power-velocity relationships during downstroke (sector 2) were strongly described by linear (Fig. 4; mean $R^2 = 0.985 \pm 0.009$) and quadratic models (mean $R^2 = 0.946 \pm 0.048$), respectively. The effective force in upstroke (sector 4) and top (sector l) also significantly decreased in a linear fashion with an increase of the pedaling rate (Fig. 4; mean $R^2 = 0.935 \pm 0.056$ and 0.875 ± 0.081, respectively).

Influence of the different functional sectors. The contribution of each functional sector expressed as a percentage of the total power output generated over the complete crank cycle is illustrated by Figure 5 for three pedaling rate (i.e., low = 80 rpm, medium = 117 rpm, i.e., close to f_{opt}, and high = 170 rpm). The mean absolute F_{eff0} and P_{max} extrapolated from linear and quadratic force-velocity and power-velocity relationships obtained during downstroke reached 1179 ± 115 N and 1250 ± 117 W, respectively. When weighting these values regarding the size of this sector relative to the entire cycle (120° for each leg), they accounted for 73.9% ± 2.1% of F_{eff0} and 73.6% ± 2.6% of P_{max}, respectively, measured on the complete cycle (Fig. 4). F_{eff0} and P_{max} obtained during upstroke represented 13.7% ± 2.1% and 10.3% ± 1.8%, respectively, of those measured on the complete cycle (Fig. 4). In the whole group, F_{eff0}, f_0, and P_{max} obtained on the complete cycle were strongly related to the same values obtained for downstroke (Fig. 5 and Table l; $P < 0.001$). Significant relationships were also found between F_{eff0} on the complete cycle and values averaged on upstroke and top (sectors 4 and 1, Table *1,* $P < 0.05$) and between P_{max} on the complete cycle and P_{max} on upstroke (sector 4, Table 1, $P < 0.05$).

Index of mechanical effectiveness. IE on the complete cycle decreased with pedaling rate. It was thoroughly described by a quadratic model ($R^2 = 0.974 \pm 0.019$; Fig. 3).
The mean maximal value of JE of the group was 79.1% ± 3.5% at a pedaling corresponding to 33.3% ± 10.8% of f_o. IE computed for the different sectors also decreased with pedaling rate according to a linear (bottom) or quadratic (top and upstroke) model except for downstroke during which IE maintained a relatively high and constant level (80%-85%) when pedaling rate ranged from 30%-35% to 70%-75% of f_o (Fig. 4). In the whole group, the absolute power output produced on the complete cycle was not correlated with JE at the three levels of pedaling rate (Table 2). At low pedaling rate (80 rpm), power output and IE were highly correlated for upstroke *(*$P < 0.01$) and moderately correlated for top *(*$P < 0.05$) (Table 2). Those relationships grew higher at intermediate pedaling rate (117 rpm) (Table 2). For high pedaling rates (170 rpm), power output and IE were significantly correlated for each sector, strongly in upstroke *(*$P < 0.001$) and highly in top and downstroke *(*$P < 0.01$) (Table 2).

DISCUSSION

Force-velocity characteristics are typically determined on conventional cycle ergometers and are based on the net force generated per revolution by the simultaneous actions of both lower limbs on both pedals (8,13,20). The instrumented pedals used in the current study provided the information necessary to examine the amount of force exerted independently by each leg in the different functional sectors of the crank pedaling cycle. These pedals also permitted to evaluate the effectiveness of force orientation on the pedal. Despite the importance of the muscle power produced during the pedal downstroke, the results confirmed the tested hypothesis of the significant influence of other phases (particularly the upstroke at pedaling rates below the optimal value) and demonstrated that pedaling technique (i.e., index of mechanical effectiveness) has an effect on the power produced during some parts of the cycle.

As for the entire crank cycle, effective force-velocity and power-velocity relationships

during downstroke were strongly described by linear and quadratic models, respectively (Fig. 4). The large contribution of downstroke demonstrated in the current study (Figs. 4 and 5) is in line with the work of Martin and Brown (19) in which the contribution of the "extension phase" (0°-180°) accounted for almost 85% of the maximal power output generated over the complete revolution. In our study, the contribution of the downstroke phase remained high and relatively constant regardless of the pedaling rate (>72%, except at the very fast cadences; Fig. 5). Moreover, all the force-velocity and power-velocity parameters (F_{eff0}, P_{max}, and f_o) obtained over the whole revolution were highly correlated with the same parameters during downstroke (Table l; $0.821 < r < 0.953$, $P < 0.001$). Thus, although the maximal power output used to describe the power-velocity characteristics depends on the complex multijoint coordination, the latter is a good predictor of the explosive muscular capabilities of lower-limb muscles involved in the downstroke phase, particularly the knee extensor muscles (2,9). It has been recently shown by the inverse dynamic technique that the hip extensors are the most powerful muscles activated in sector 2 during sprint cycling (19). On the basis of both these former studies and the results of the present experiment, it appears that force-velocity cycling test informs the muscle function of the hip extensors, knee extensors, and to a lesser extent ankle extensors. Nevertheless, more than 25% of the total power output was produced during phases other than the propulsive phase, which highlights the important contribution of the other parts of the crank cycle (Fig. 5).

The effective force in upstroke (sector 4) significantly decreased in a linear fashion with pedaling rate and became negative at 169 ± 18 rpm (i.e., 71.5% ± 8% of f_0; Fig. 4). All the results regarding the mechanical output during upstroke indicate the important implication of this flexion phase, especially at high force levels and slow pedaling rates (>10% of the total power; Fig. 5). This contribution is corroborated by F_{eff0} and P_{max} values obtained during upstroke. These results confirm previous findings (2) that during maximal effort (in contrast to the submaximal exercise), pulling on the pedal significantly contributes to power production during upstroke. The present study showed a decrease in the leg flexion contribution, which became negative at very high cadences (Fig. 4). This contrants previous work that found a quasi-constant participation of the leg flexion phase at cadences below 120 rpm (2). Moreover, F_{eff0} and P_{max} over the complete revolution and during upstroke were significantly related ($P < 0.05$; Table 1). Thus, the force and the power characteristics of the muscles acting in this part of the cycle play a nonnegligible vole in the results classically obtained from the force-velocity test (i.e., on the complete cycle). Along this line, Martin and Brown (19) recently demonstrated that during a sprint performed at 120 rpm (here corresponding almost to P_{max}), knee flexion produced nearly the same power as knee extension: almost 20% of the muscular power during a complete revolution. The discrepancy concerning the contribution of the upstroke between the previous work and our findings (approximately 10%) could be partly explained by the difference in the angular sector (i.e., 180°-360° for Martin and Brown (19), 210°-330° in the present study). Moreover, the previous study (19) took into consideration the influence of the nonmuscular forces (linked to the inertial properties and changes in potential energy of the lower-limb segments) on the total resultant pedal force. This was not the case in the present study, leading F_{eff} to overestimate the force actually produced by the lower-limb muscles in the downstroke phase and to underestimate the muscle force produced in the upstroke phase. Finally, it could explain, at least partially, the difference in the maximal velocity characteristics (f_0) reported in the present study between downstroke and upstroke.

The contributions of the two transition phases (top and bottom) were not so significant (Fig. 5), and changes in force and power as a function of pedaling rate differed from the linear and quadratic models (Fig. 4). Even if linear force-velocity and quadratic power-velocity relationships around the top of the pedaling cycle (top) were significant, the mean R^2 was low (Fig. 4). A slightly significant relationship existed between F_{eff0} measured in top and F_{eff0} measured over the complete cycle (Table 1). However, the contribution of this phase to the total force remained limited, as F_{eff0} in this sector amounted only 6.3% ± 0.7% of the total F_{eff0} (Fig. 5). The relative stability of effective force with pedaling rate around the BDC (bottom) is not consistent with the traditional conception of the muscular force-velocity relationship (1,4,8,14,15,21,22,35). Therefore, the mechanical production in this phase failed to explain the variance of force and/or power measured during the complete cycle (Table 1). The increase of

power at high pedaling rates in this phase (Figs. 4 and 5) could result from a forward shift in the force profile along the crank cycle (Fig. 2). Some authors have previously reported a higher torque near the end of the downward pedal motion (between 154° and 176°) at high velocities rather than at low velocities (4,5). This is in agreement with the problem of activation dynamics pointed out by Samozino et al. (28) during a similar sprint cycling test. Because of the electromechanical delay (estimated between 40 and 100 ms in this context), the force production is shifted later in the crank cycle when pedaling rate is increased (28). Thus, force could be produced during a less effective sector. In addition, in these transition phases, the influence of forces from non-muscular origins may be large (4,5,25). Therefore, based only on our results, it is difficult to conclude whether the force production in both transition phases reflects a significant influence of these parameters and/or is related to actual muscle capability including (i) the strength of biarticular knee flexors or hip extensors near the BDC (bottom), the strength of the hip flexors just before the TDC (top), and the strength of the hip and knee extensors just alter the TDC; and (ii) the capacity of these biarticular muscles to transfer energy between joints and to control the direction of force production during critical sectors (33). Finally, it was interesting to note a high interindividual variability in power production during these two phases as well as in upstroke especially at high pedaling rates (Figs. 4 and 5). These findings support previous work of Hug et al. (17), who reported high intersubject variability in the mechanical patterns during top in a submaximal exercise.

To the best of our knowledge, values of IE during an all-out cycling exercise have not been previously reported in the literature. Previous investigations have reported values between 30% and 65% by focusing only on submaximal exercise (26,29,36). These studies demonstrated a significant increase in IE measured over the complete cycle with an increase of workload but a reduced IE at a given power output as cadence increased. In the present study, values for the complete revolution (between 76% ± 4% and 73% ± 5 % from 30% to 50% of f_0: —70 to 120 rpm; Fig. 3) were much higher than those previously reported at similar cadences. This result extends on previous findings that an increase in exercise intensity is associated with an optimization of the total force applied to the pedals (26,29,36), especially in these sprint conditions. Indeed, power output ranged here from 900 to 1150 W, which was four to six times greater than submaximal powers reported in the literature. Compared with submaximal exercise, the mechanical effectiveness in sprint cycling appeared slightly higher in the downstroke and much higher in the upstroke for pedaling rates up to the optimal value (24,27). The significant reduction in IE to 35% ± 5% at velocities around 80% of f_0 (-190 rpm; Fig. 3) highlights the difficulty of efficiently orientating the force on pedals at a high pedaling rate. This could be largely explained by the decrease of IE in upstroke, whereas IE in downstroke remained at a constant high level except for pedaling rates superior to 75% of f_0. The typical decrease of IE over the complete cycle (and hence in bottom and upstroke; Figs. 3 and 4) could be interpreted as a reduced capacity of the lower-limb muscles to produce an efficient resultant muscle component of the force on the pedal. This could be attributed to activation dynamics as the pedaling rate increases (25,34). Reductions in IE could partially explain the descending portion of the power-velocity relationship when pedaling higher than fo_r*

The absence of a significant relationship between the power output and IE over the complete cycle (Table 2) disproves our initial hypothesis that IE is an explanatory factor for the differences in power characteristics of the subjects. This is largely explained by the fact that during the powerful downstroke phase, IE remained at a constant high level with low interindividual variability (Fig. 4). On the other hand, high correlations between power output and IE were obtained for the whole sample in top and upstroke at all pedaling rates and in all parts of the cycle at high pedaling rate (i.e., 170 rpm) (Table 2). However, the increase in the non-muscular pedal force component and of its influence at a very fast pedaling rate (4,25) certainly accounts for the smaller decrease or the increase of the total resultant force. This change in resultant force subsequently accounts for the decrease in IE over the different phases of the crank cycle. This point avoids a shortcut by considering a direct link between the index of mechanical effectiveness and the ability of the muscles to be activated in the optimal manner (relevant to the coordination strategy and the technical aspect of pedaling).

In conclusion, this study confirms that force-velocity and power-velocity characteristics in cycling typify the function of muscles responsible for pushing on the pedal, especially the hip and the knee extensors. The results showed an important positive contribution from the upstroke phase (almost 14% of maximal force on the entire cycle). Significant relationships

also existed between maximal force and power produced in the upstroke phase and those obtained on the complete revolution. This clearly indicates that data from all-out cycling exercise should also reflect the muscular capability of muscles to actively participate to the pedal upstroke. It appears therefore relevant to include a measurement of the contribution of both flexion and extension phases in future cycling force-velocity testing procedures. The index of effectiveness does not have a great influence on power production over the complete cycle. However, IE remains a significant explanatory factor for differences in power production during the upstroke and around the TDC at pedaling rates under the optimal value (f_{opt}) and during all phases at higher cadences. Further studies using inverse dynamics (including calculation of both muscular and non-muscular components) and measurement of EMG activity in different expert populations (i.e., endurance and sprint cyclists) may better characterize the involvement of each functional phases and muscle groups. Testing the elite athletes would also help clarify the role of the pedaling technique and the ability of subjects to efficiently orientate the resultant force at the shoe-pedal interface.

This study was funded in part by "La fondation d'entreprise de la Française Des Jeux". The authors are grateful to the subjects for having agreed to participate in this study.

REFERENCES

1. Arsac LM, Belli A, Lacour JR. Muscle function during brief maximal exercise: accurate measurements on a friction-loaded cycle ergometer. *Eur J Appl Physiol Occup Physiol.* 1996;74(1-2):100-6.
2. Beelen A, Sargeant AJ, Wijkhuizen F. Measurement of directional force and power during human submaximal and maximal isokinetic exercise. *Eur J Appl Physiol Occup Physiol.* 1994; 68(2):177-81.
3. Bosco C, Luhtanen P, Komi PV. A simple method for measurement of mechanical power in jumping. *Eur J Appl Physiol Occup Physiol.* 1983;50(2):273-82.
4. Buttelli O, Vandewalle H, Peres G. The relationship between maximal power and maximal torque-velocity using an electronic ergometer. *Eur J Appl Physiol Occup Physiol.* 1996;73(5): 479-83.
5. Capmal S, Vandewalle H. Torque-velocity relationship during cycle ergometer sprints with and without toe clips. *Eur J Appl Physiol Occup Physiol.* 1997;76(4):375-9.
6. Coyle EF, Feltner ME, Kautz SA, et al. Physiological and biomechanical factors associated with elite endurance cycling performance. *Med Sci Sports Exerc.* 1991;23(1):93-107.
7. Dorel S, Drouet JM, Couturier A, Champoux Y, Hug F. Changes of pedaling technique and muscle coordination during an exhaustive exercise. *Med Sci Sports Exerc.* 2009;41(6):1277-86.
8. Dorel S, Hautier CA, Rambaud O, et al. Torque and powervelocity relationships in cycling: relevance to track sprint performance in world-class cyclists. *Int J Sports Med.* 2005;26(9): 739-46.
9. Driss T, Vandewalle H, Le Chevalier JM, Monod H. Forcevelocity relationship on a cycle ergometer and knee-extensor strength indices. *Can J Appl Physiol.* 2002;27(3):250-62.
10. Drouet JM, Champoux Y, Dorel S. Development of multiplatform instrumented force pedals for track cycling. In: Estivalet M, Brisson P, editors. *The Engineering of Sport 7.* Paris: Springer; 2008. p. 263-71.
11. Ericson M. On the biomechanics of cycling: a study of joint and muscle load during exercise on the bicycle ergometer. *Scand J Rehabil Med Suppl.* 1986;16:1-43.
12. Gregor RJ, Cavanagh PR, LaFortune M. Knee flexor moments during propulsion in cycling-a creative solution to Lombard's paradox. *J Biomech.* 1985;18(5):307-16.
13. Hautier CA, Belli A, Lacour JR. A method for assessing muscle fatigue during sprint exercise in humans using a friction-loaded cycle ergometer. *Eur J Appl Physiol Occup Physiol.*

1998;78(3): 231-5.
14. Hautier CA, Linossier MT, Belli A, Lacour JR, Arsac LM. Optimal velocity for maximal power production in non-isokinetic cycling is related to muscle fibre type composition. *Eur J Appl Physiol Occup Physiol.* 1996;74(1-2):114-8.
15. Hintzy F, Belli A, Grappe F, Rouillon JD. Optimal pedalling velocity characteristics during maximal and submaximal cycling in humans. *Eur J Appl Physiol Occup Physiol.* 1999;79(5): 426-32.
16. Hug F, Dorel S. Electromyographic analysis of pedaling: a review. *J Electromyogr Kinesiol.* 2009;19(2):182-98.
17. Hug F, Drouet JM, Champoux Y, Couturier A, Dorel S. Interindividual variability of electromyographic patterns and pedal force profiles in trained cyclists. *Eur J Appl Physiol.* 2008;104(4): 667-78.
18. LaFortune M, Cavanagh PR. Effectiveness and efficiency during bicycle riding. In: Matsui H, Kobayashi K, editors. *Biomechanics VIIB: International Series on Biomechanics 4B.* Champaign (IL): Human Kinetics; 1983. p. 928-36.
19. Martin JC, Brown NA. Joint-specific power production and fatigue during maximal cycling. *J Biomech.* 2009;42(4):474-9.

20. Martin JC, Spirduso WW. Determinants of maximal cycling power: crank length, pedaling rate and pedal speed. *Eur J Appl Physiol.* 2001 ;84(5):413-8.
21. Martin JC, Wagner BM, Coyle EF. Inertial-load method determines maximal cycling power in a single exercise bout. *Med Sci Sports Exerc.* 1997;29(11):1505-12.
22. Morin JB, Hintzy F, Belli A, Grappe F. Force-velocity relationships and sprint running performances in trained athletes. *Sci Sports.* 2002 ;17(2):78-85 .
23. Mornieux G, Guenette JA, Sheel AW, Sanderson DJ. Influence of cadence, power output and hypoxia on the joint moment distribution during cycling. *Eur J Appl Physiol.* 2007;102(1): 11-8.
24. Mornieux G, Stapelfeldt B, Gollhofer A, Belli A. Effects of pedal type and pull-up action during cycling. *Int J Sports Med.* 2008; 29(10):817-22.
25. Neptune RR, Herzog W. The association between negative muscle work and pedaling rate. *J Biomech.* 1999;32(10):1021-6.
26. Patterson RP, Moreno MI. Bicycle pedalling forces as a function of pedalling rate and power output. *Med Sci Sports Exerc.* 1990;22(4):512-6.
27. Rossato M, Bini RR, Carpes FP, Diefenthaeler F, Moro AR. Cadence and workload effects on pedaling technique of welltrained cyclists. *Int J Sports Med.* 2008;29(9):746-52
28. 28. Samozino P, Horvais N, Hintzy F. Why does power output decrease at high pedaling rates during sprint cycling? *Med Sci Sports Exerc.* 2007;39(4):680-7.

29. Sanderson DJ. The influence of cadence and power output on the biomechanics of force application during steady-rate cycling in competitive and recreational cyclists. *J Sports Sci.* 1991;9(2): 191-203.
30. Sanderson DJ, Black A. The effect of prolonged cycling on pedal forces. *J Sports Sci.* 2003;21(3):191-9.
31. Sanderson Di, Hennig EM, Black AH. The influence of cadence and power output on force application and in-shoe pressure distribution during cycling by competitive and recreational cyclists. *J Sports Sci.* 2000;18(3):173-81.
32. Sargeant AJ, Hoinville E, Young A. Maximum leg force and power output during short-term dynamic exercise. *J Appl Physiol.* 1981;51(5):1175-82.
33. van Ingen Schenau GJ, Boots Pi, de Groot G, Snackers RJ, van Woensel WW. The constrained control of force and position in multi-joint movements. *Neuroscience.* 1992;46(1):197-207.
34. van Soest O, Casius LJ. Which factors determine the optimal pedaling rate in sprint cycling?

Med Sci Sports Exerc. 2000; 32(11):1927-34.
35. Vandewalle H, Peres G, Heller J, Panel .1›, Monod H. Forcevelocity relationship and maximal power on a cycle ergometer. Correlation with the height of a vertical jump. *Eur J Appl Physiol Occup Physiol.* 1987;56(6):650-6.
36. Zameziati K, Mornieux G, Rouffet D, Belli A. Relationship between the increase of effectiveness indexes and the increase of muscular efficiency with cycling power. *Eur J Appl Physiol.* 2006;96(3):274-81.

TABLE 1. - Correlation between the maximal force (F_{eff0}), the maximal pedaling rate (f_0), and the maximal power output *(P_{max}.)* measured on the complete cycle for each subject and the same values resulting from the force-velocity and the power-velocity relationships obtained in each functional sectors *(N*= 14).

	Complete Cycle	
	r	*P*
F_{eff0}		
Top (sector 1)	0.626	0.017
Downstroke (sector 2)	0.953	<0.001
Bottom (sector 3)	–	–
Upstroke (sector 4)	0.627	0.016
f_0		
Top (sector 1)	0.068	NS
Downstroke (sector 2)	0.821	<0.001
Bottom (sector 3)	–	–
Upstroke (sector 4)	0.077	NS
P_{max}		
Top (sector 1)	0.116	NS
Downstroke (sector 2)	0.927	<0.001
Bottom (sector 3)	–	–
Upstroke (sector 4)	0.566	0.035

Values concerning correlation for bottom (sector 3) do not exist because force and power output changes with pedaling rate failed to be described by a classical mathematical model (see Fig. 3).
NS, not statistically significant.

TABLE 2. - Correlation between the power output and the index of mechanical effectiveness on the complete cycle and during each of the functional sectors in three pedaling conditions of the power-velocity relationship (low = 80 rpm, medium = 117 rpm, and high = 170 rpm) *(N*= 14).

	Index of Mechanical Effectiveness	
Power Output	*r*	*P*
80 rpm		
Complete cycle	0.360	NS
Top (sector 1)	0.625	0.017
Downstroke (sector 2)	0.245	NS
Bottom (sector 3)	0.239	NS
Upstroke (sector 4)	0.764	0.004
117 rpm ($\sim f_{opt}$)		
Complete cycle	0.264	NS
Top (sector 1)	0.750	0.002
Downstroke (sector 2)	0.410	NS
Bottom (sector 3)	0.031	NS
Upstroke (sector 4)	0.852	<0.001
170 rpm		
Complete cycle	0.476	NS
Top (sector 1)	0.685	0.007
Downstroke (sector 2)	0.709	0.005
Bottom (sector 3)	0.535	0.049
Upstroke (sector 4)	0.977	<0.001

NS, not statistically significant.

FIGURE 1 - Representation of the instrumented pedals, the forces applied on the right pedal on a sagittal plan, and the different angular sectors. Total force (F_{tot}) produced at the shoe-pedal interface is decomposed in two components: a) an effective force (F_{eff}) acting perpendicularly to the crank and b) an ineffective component *(F_i)* acting along the crank.

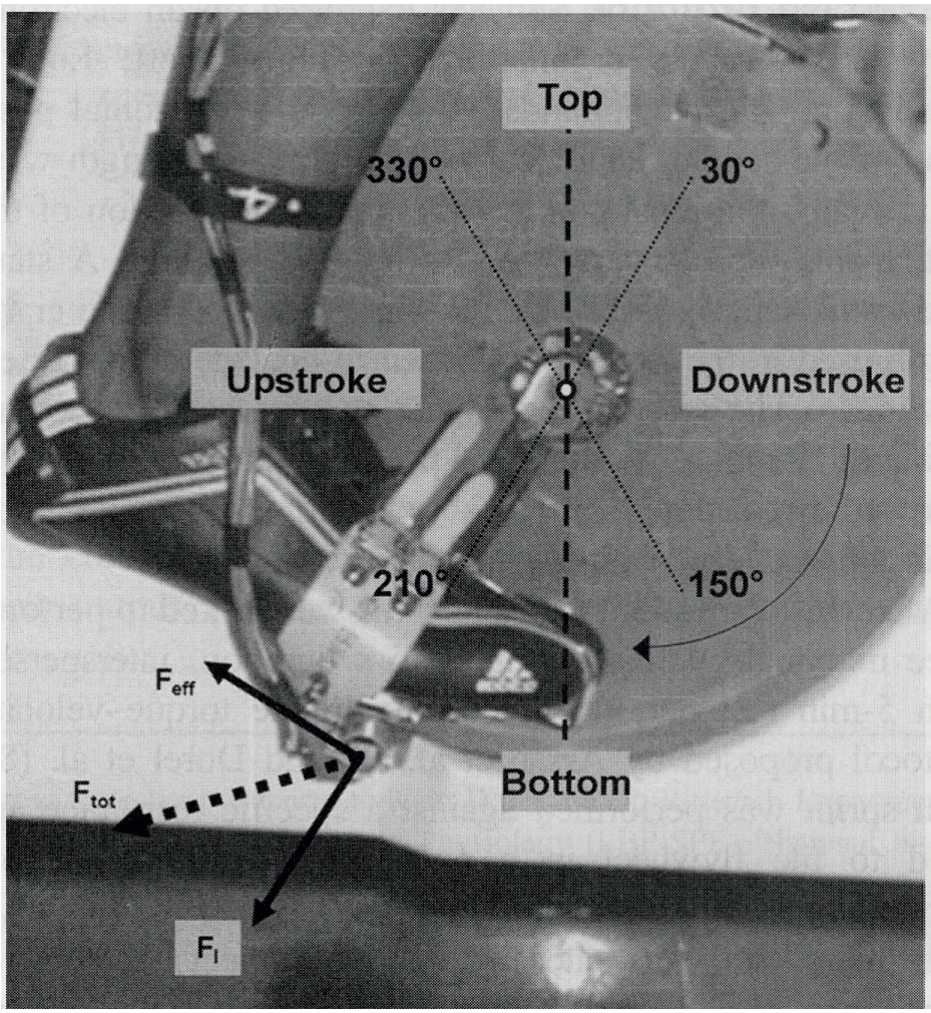

FIGURE 2 - Example of the total and effective force produced on the left pedal during a complete crank revolution at low (A), medium (B), and high (C) pedaling rate. 1: Top, sector 1; 2: downstroke, sector 2; 3: bottom sector 3; 4: upstroke, sector 4. Force and power characteristics of the subject (i.e., taking both legs into account): F_{eff0} = 1187 N, f_0 = 232 rpm,f_{opt} = 117 rpm, P_{max}. = 1260 W.

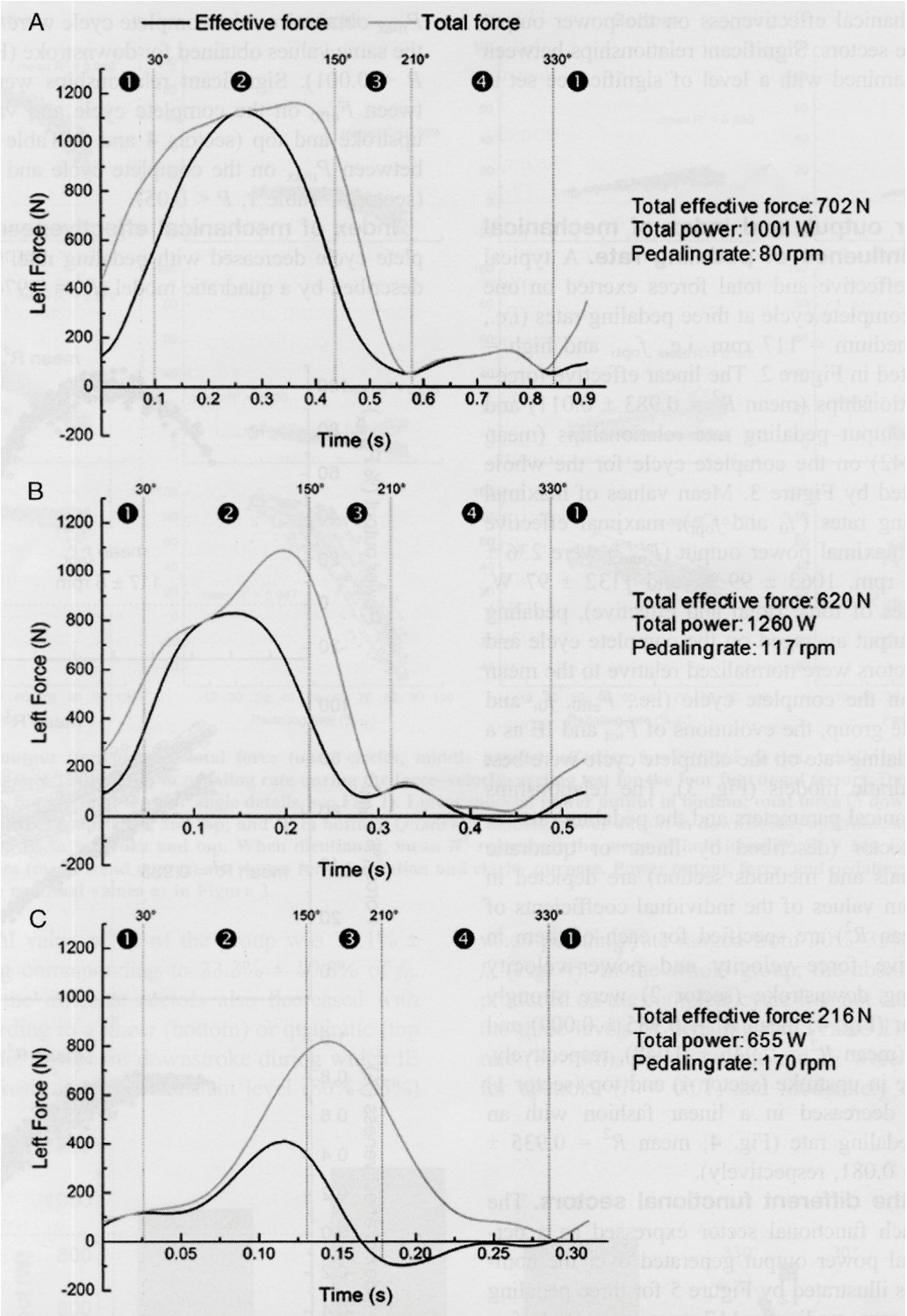

FIGURE 3 - Power output (top panel), total force (open circles, middle panel), effective force (filled circles, middle panel), and index of effectiveness (bottom panel) in relation to pedaling rate during the force-velocity cycling test. Data result from the three sprints of 5-s duration. For power output (quadratic model), total force (quadratic model), effective force (linear model), and index of effectiveness (quadratic model), the mean of individuals R^2 *(N* = 14) are mentioned on graphs. Gray limes (individual models) and black limes (mean trend curves) are shown for information and clarity purpose. Power output, force, and pedaling rate are normalized relatively to their maximal values P_{max}, $F_{eff0,}$ and f_0.

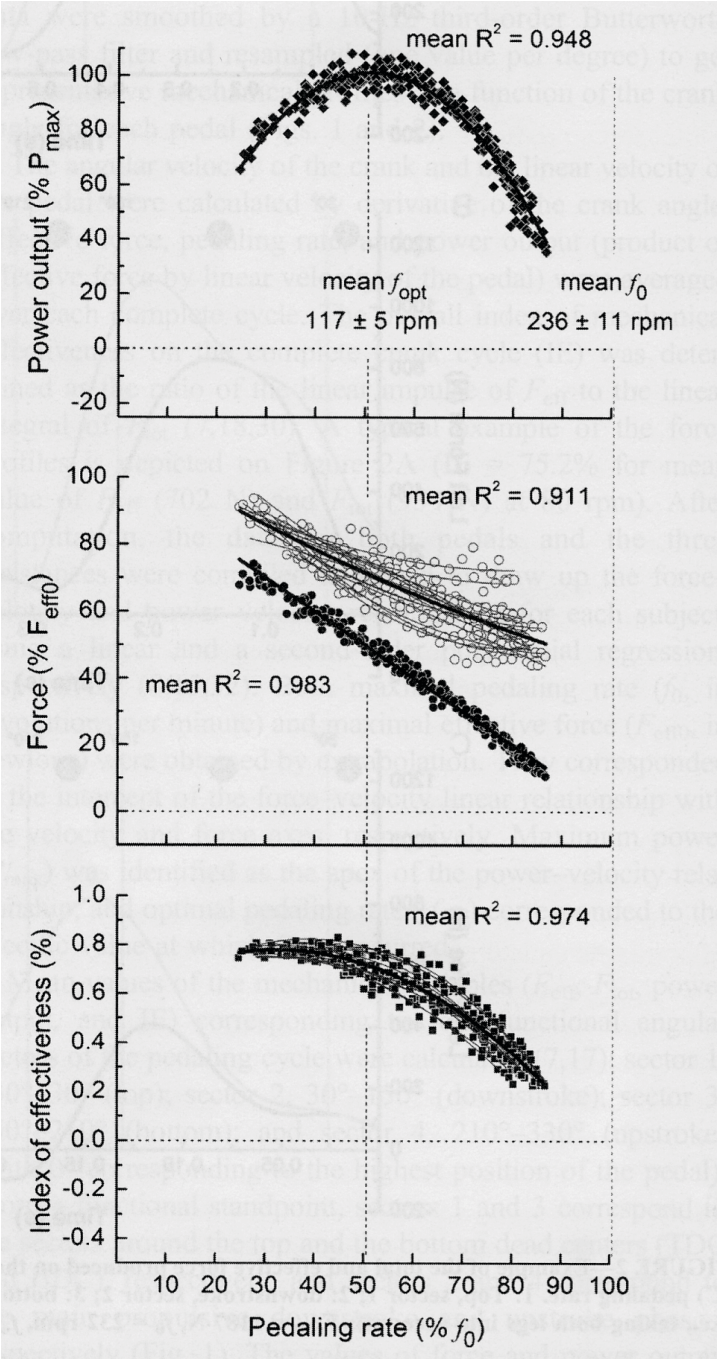

FIGURE 4 - Power output (top panels), total force (open circles, middle panels), effective force (filled circles, middle panels), and index of effectiveness (bottom panels) in relation to pedaling rate during the force—velocity cycling test for the four functional sectors. Data are averaged over downstroke, upstroke, bottom, and top (for angle details, see Fig. 1). Linear models: power output in bottom; total force in downstroke and bottom; effective force in downstroke, upstroke, and top; and IE in bottom. Quadratic models: power output in downstroke, upstroke, and top; total force in upstroke and top; and IE in upstroke and top. When mentioned, mean R^2 represents the mean of individual R^2 *(N* = 14). Gray limes (individual models) and black limes (mean trend curves) are shown for information and clarity purpose. Power output, force, and pedaling rate are normalized relatively to the same maximal values as in Figure 3.

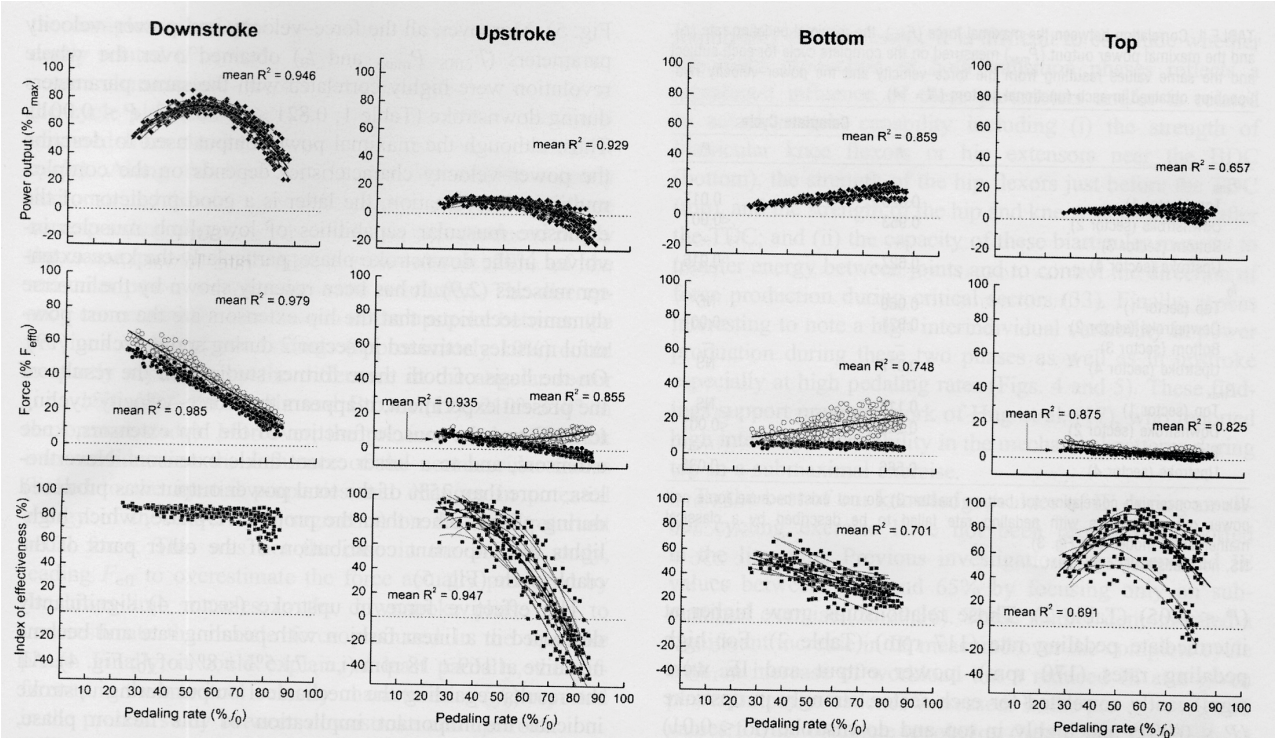

FIGURE 5 - Mean power output produced during each of the four functional sectors in three pedaling conditions of the force-velocity relationship. Numerical values ± SD in histograms are expressed as the percentage of total power output produced on the entire cycle (i.e., contribution). S1: top; S2: downstroke; S3: bottom; S4: upstroke.